Biochimica et Biophysica Acta 1842 (2014) 613–622

Contents lists available at ScienceDirect

Biochimica et Biophysica Acta

journal homepage: www.elsevier.com/locate/bbadis

HO-1 up-regulation: A key point in high-risk neuroblastoma resistance to bortezomib ☆

Anna Lisa Furfaro [a], Sabrina Piras [a], Mario Passalacqua [a], Cinzia Domenicotti [a], Alessia Parodi [b], Daniela Fenoglio [b], Maria Adelaide Pronzato [a], Umberto Maria Marinari [a], Lorenzo Moretta [c], Nicola Traverso [a], Mariapaola Nitti [a,*]

[a] Department of Experimental Medicine, University of Genoa, 2, L.B. Alberti Street, I-16132 Genoa, Italy
[b] Center of Excellence for Biomedical Research, Department of Internal Medicine, University of Genoa, 16132 Genoa, Italy
[c] Giannina Gaslini Institute, 16147 Genoa, Italy

ARTICLE INFO

Article history:
Received 31 July 2013
Received in revised form 17 December 2013
Accepted 19 December 2013
Available online 28 December 2013

Keywords:
Redox signaling
Chemoresistance
Heme oxygenase-1
Neuroblastoma

ABSTRACT

High-risk neuroblastoma (NB) is characterized by the development of chemoresistance, and bortezomib (BTZ), a selective inhibitor of proteasome, has been proposed in order to overcome drug resistance. Considering the involvement of the nuclear factor-erythroid-derived 2-like 2 (Nrf2) and heme oxygenase-1 (HO-1) in the antioxidant and detoxifying ability of cancer cells, in this study we have investigated their role in differently aggressive NB cell lines treated with BTZ, focusing on the modulation of HO-1 to improve sensitivity to therapy. We have shown that MYCN amplified HTLA-230 cells were slightly sensitive to BTZ treatment, due to the activation of Nrf2 that led to an impressive up-regulation of HO-1. BTZ-treated HTLA-230 cells down-regulated p53 and up-regulated p21, favoring cell survival. The inhibition of HO-1 activity obtained by Zinc (II) protoprophyrin IX (ZnPPIX) was able to significantly increase the pro-apoptotic effect of BTZ in a p53- and p21-independent way. However, MYCN non-amplified SH-SY5Y cells showed a greater sensitivity to BTZ in relation to their inability to up-regulate HO-1. Therefore, we have shown that HO-1 inhibition improves the sensitivity of aggressive NB to proteasome inhibition-based therapy, suggesting that HO-1 up-regulation can be used as a marker of chemoresistance in NB. These results open up a new scenario in developing a combined therapy to overcome chemoresistance in high-risk neuroblastoma.

1. Introduction

Neuroblastoma (NB) is the most common extra-cranial solid tumor in childhood. It accounts for 8–10% of all pediatric cancers and 15% of childhood cancer mortality [1]. One of the clinical hallmarks of neuroblastoma is heterogeneity, varying from the highly aggressive chemoresistant disease to the spontaneous regression in infants [2]. Despite advances in the treatment of other childhood tumors, high-risk neuroblastoma remains one of the most difficult cancers to cure with long-term survival still less than 40%. A typical feature of high-risk disease is MYCN amplification, which occurs in around 20–25% of neuroblastoma, associated with rapid tumor progression, chemoresistance and poor prognosis [3].

The availability of antioxidants is recognized as one of the critical mechanisms able to provide cancer cells with resistance to anticancer therapies [4]. In drug resistance, nuclear factor-erythroid-derived 2-like 2 (Nrf2) is reported to play a key role [5]. Nrf2 is activated in response to electrophylic stimuli and oxidative stress and regulates the expression of many antioxidant and detoxifying genes involved in the development of chemoresistance [6]. Among Nrf2 target genes, heme oxygenase-1 (HO-1) is considered a master regulator of antioxidant response. Heme oxygenase is the first and rate-limiting enzyme in the degradation of heme into biliverdin, carbon monoxide (CO), and free iron [7]. HO-1, the inducible form of the HO system, is a 32-kDa stress protein and is present at low levels in most mammalian tissues [8]. Its expression is induced by a wide variety of stress stimuli, including its substrate, heavy metals, UV irradiation, reactive oxygen species (ROS), nitric oxide, and inflammatory cytokines [9–11]. HO-1 and its metabolic products are involved in the maintenance of cellular homeostasis and play a key role in the adaptive response to cellular stress [12]. Recent experimental evidence has shown the involvement of HO-1 in cancer cell biology, with a dual role. On one hand, HO-1 protects healthy cells from transformation into neoplastic cells by counteracting ROS mediated

* Corresponding author. Tel.: +39 010 3538831; fax: +39 010 3538836.
E-mail addresses: annalisa.furfaro@unige.it (A.L. Furfaro), piras.sabri@tiscali.it (S. Piras), Mario.Passalacqua@unige.it (M. Passalacqua), Cinzia.Domenicotti@unige.it (C. Domenicotti), alessiaparodi@yahoo.it (A. Parodi), Daniela.Fenoglio@unige.it (D. Fenoglio), maidep@unige.it (M.A. Pronzato), umm@unige.it (U.M. Marinari), Lorenzo.Moretta@ospedale-gaslini.ge.it (L. Moretta), Nicola.Traverso@unige.it (N. Traverso), Mariapaola.Nitti@unige.it (M. Nitti).

0925-4439/$ – see front matter © 2013 The Authors. Published by Elsevier B.V. All rights reserved.
http://dx.doi.org/10.1016/j.bbadis.2013.12.008

carcinogenesis. On the other hand, HO-1 protects cancer cells, improving their survival and their resistance to anticancer treatment [13]. High levels of HO-1 have been observed in various human solid tumors (e.g. renal, prostatic and pancreatic) [14–16]. Moreover, HO-1 expression in tumor cells can be further increased by anticancer treatments (chemo-, radio-, and photodynamic therapy) [16] and it has been hypothesized that HO-1 and its products may have an important role in the development of a resistant phenotype [17,18].

Among the new therapeutic strategies designed to overcome cancer cell resistance, the use of proteasome inhibitors has been proposed [19,20].

Bortezomib (BTZ), a selective and reversible inhibitor of the 26S proteasome, the major intracellular pathway of protein degradation, has shown impressive clinical results in anticancer therapeutic approaches. BTZ was approved in 2004 by the US FDA for the treatment of multiple myeloma [21]. Recent experimental evidence has shown that BTZ treatment is able to overcome cancer cell resistance in different solid tumors [22].

In this study we have investigated the effects of bortezomib treatment on neuroblastoma cell lines. We used two NB cell lines: SH-SY5Y, MYCN non-amplified, and HTLA-230, MYCN amplified, in order to mimic two differently aggressive conditions and to compare their sensitivity to bortezomib. In particular, Nrf2/HO-1 pathway has been studied in both cell lines, focusing on the effect of HO-1 modulation to improve BTZ efficacy.

2. Materials and methods

2.1. Cell culture and treatments

MYCN non-amplified SH-SY5Y cells and MYCN amplified, stage IV, HTLA-230 human neuroblastoma cells were obtained from Prof. V. Pistoia (G. Gaslini Institute, Genoa, Italy). Both cell lines were maintained in RPMI 1640 medium (Euroclone, Milan, Italy) supplemented with 10% FBS (Euroclone), 2 mM glutamine (Sigma-Aldrich, Milan, Italy), 1% penicillin/streptomycin (Sigma-Aldrich) and 1% amphotericin B (Sigma-Aldrich), at 37 °C in a 5% CO_2 humid atmosphere and subcultured every 4 days at 1:5.

Both cell lines were treated for 24 h with 5, 10, 20 and 40 nM bortezomib (Santa Cruz Biotechnology, Santa Cruz, CA, USA). Some samples were co-treated with 2.5 μM Zinc (II) protoporphyrin IX (Sigma-Aldrich).

2.2. MTT assay

Cell viability was evaluated by using 3-(4,5-dimethyl-thiazol-2-yl)-2,5-diphenyltetrazolium bromide (MTT, Sigma-Aldrich) assay. Cells were plated in 96-well plates and after 24 h of bortezomib treatment, incubated with 5 μg/ml MTT for 3 h at 37 °C. Insoluble formazan salts were dissolved in DMSO. The absorbance at 570 nm was measured with a spectrophotometric plate reader (EL-808 BIO-TEK Instruments Inc.). Mean values from each treatment were calculated as a percentage relative to the untreated control cells.

2.3. Detection of cells death by FACS analysis

After treatment, cells were stained with Annexin V-FITC and Propidium Iodide according to the manufacturer's instructions (BioVision, Mountain View, CA, USA). Stained samples were analyzed by flow cytometry using a FACSCanto II flow cytometer (Becton Dickinson Italia, BD, Milan, Italy) equipped by FacsDiva software (BD). At least 10,000 events were analyzed. Each experiment was performed three times.

2.4. Cell proliferation assay

Cell proliferation was evaluated by staining cells with carboxyl fluorescein succinimidyl ester (CFDA-SE, Invitrogen, Milan, Italy), a lipophilic dye that reacts with amino groups on peptides and proteins forming a stable amide bond, and detection by flow cytometry analysis [18,23]. Cells were seeded in six-well plates, washed and incubated with 5 μM CFDA-SE in 10 mM PBS in the dark at 37 °C in 5% CO_2 for 5 min. At the end of incubation, the cells were washed three times with 10 mM PBS supplemented with 1% FBS. Then, the samples were exposed to the treatments described in Section 2.1. After 24 h cells were washed and scraped-off in PBS and the intensity of CFDA-SE fluorescence was evaluated by flow cytometry. The proliferation of CFDA-SE-labeled cells was estimated by the progressive halving of cellular fluorescence as every cell division was completed. Samples were analyzed using a FACSCanto II flow cytometer and FacsDiva software (BD). The flow cytometry data files were analyzed using the Proliferation Wizard module of the ModFit LT 3.2 software (Verity Software House Inc., Topsham, ME, USA). Each experiment was performed three times.

2.5. RNA extraction and RT-PCR

Total RNA was extracted using TRIZOL reagent (Invitrogen) according to the manufacturer's instructions and was then reverse transcribed into cDNA by random hexamer primers and SuperScript™ II Reverse Transcriptase (Invitrogen). Amplification of cDNA by polymerase chain reaction was performed using Platinum Taq DNA Polymerase (Invitrogen) and specific primers for human GCLC, GCLM, HO-1, NQO1, x-CT, p21 and MYCN. Ribosomal 18S expression was used as the housekeeping gene. Primer sequences used (Tib Mol Biol, Genoa, Italy) were: **GCLC** Fw 5′ ATG GAG GTG CAA TTA ACA GAC 3′; GCLC Rv 5′ ACT GCA TTG CCA CCT TTG CA 3′ (206 bp); **GCLM** Fw 5′ CCA GAT GTC TTG GAA TGC 3′; GCLM Rv 5′ TGC AGT CAA ATC TGG TGG 3′ (408 bp); **HO-1** Fw 5′ GCT CAA CAT CCA GCT CTT TGA GG 3′; HO-1 Rv 5′ GAC AAA GTT CAT GGC CCT GGG A 3′ (284 bp); **NQO1** Fw 5′ CAC TGA TCG TAC TGG CTC A 3′; NQO1 Rv 5′ GCA GAA TGC CAC TCT GAA T 3′ (516 bp); **x-CT** Fw 5′ CGT CCT TTC AAG GTG CCA CTG 3′; x-CT Rv 5′ TGT CTC CCC TTG GGC AGA TTG 3′ (295 bp); **p21** Fw 5′ GTC CAG CGA CCT TCC TCA TCC A 3′; p21 Rv 5′ CCA TAG CCT CTA CTG CCA CCA TC 3′ (108 bp); **MYCN** Fw 5′ CCT GAG CGA TTC AGA TGA TG 3′; MYCN Rv 5′ GGC TCA AGC TCT TAG CCT TT 3′ (337 bp); **18s** Fw 5′ GGG GCC CGA AGC GTT TAC T 3′; 18s Rv 5′ GGT CGG AAC TAC GAC GGT ATC 3′ (296 bp). PCR products were separated by electrophoresis on 2% agarose gel pre-stained with ethidium bromide, visualized under UV light and quantified by densitometric analysis by using a specific software (GelDoc, BioRad, Milan, Italy).

2.6. Total protein extraction

Total protein extraction was performed using RIPA buffer as previously described [18].

2.7. Subcellular fractioning

Cytosolic and nuclear protein extraction was performed by using Nuclear Extract Kit (Active Motif, Belgium) following the manufacturer's instruction. Protein concentration of each subcellular fraction was measured using the BCA test (Pierce, Thermo Fisher Scientific, Rockford, USA).

2.8. Western Blot

Proteins were denatured in Laemmli buffer and then subjected to 10% or Any-kD SDS-polyacrylamide gel electrophoresis 200 V for 50 min (Mini Protean TGX Gel, Bio-Rad, Milan, Italy), followed by electroblotting (100 V for 50 min) on PVDF membrane (Pierce).

Immunodetection was performed using anti Nrf2 antibody (sc-722, Santa Cruz Biotech.), anti Keap-1(H436, Cell Signaling Technology, Boston, MA, USA), anti p53 (sc-126, Santa Cruz Biotech.), anti HO-1 (ab-13248, Abcam Cambridge, UK), anti Ubiquitin (sc-8017, Santa Cruz Biotech.), anti p21(sc-6246, Santa Cruz Biotech.) and anti N-myc (OP13,OP13L Calbiochem, Merck Millipore, Italy).

After incubation with secondary antibody, the specific bands were detected by means of an enhanced chemiluminescence system (Pierce). The membranes were stripped using Re-blot plus solution (Chemicon International, CA, USA) and re-probed with anti tubulin (ab56676, Abcam) and anti laminin B1 (ab20396, Abcam). Developed films were analyzed using a specific software (GelDoc, Bio-Rad, Milan, Italy).

2.9. Electrophoretic mobility shift assay

ARE oligonucleotide was synthesized by TIB Molbiol using a commonly used sequence (5′-Tgg ggA ACC TgT gCT gAg TCA CTg gAg) [24].

The oligonucleotide was labeled using [γ-32P]ATP (PerkinElmer, USA) and T4 polynucleotide kinase (New England BioLabs, UK) and purified on Quick Spin Columns (G-25 Sephadex comumns) (Roche, Milan, Italy).

Equal amounts (2 μg) of nuclear extract proteins were added to a reaction mixture containing 20 μg of BSA, 2 μg of poly (dI-dC) (Pierce), 2 μl of buffer A (20 mM HEPES pH 7.9, 20% glycerol, 100 mM KCl, 0.5 mM EDTA, 0.25% Nonidet P-40, 2 mM DTT, and 0.1% PMSF), 4 μl of

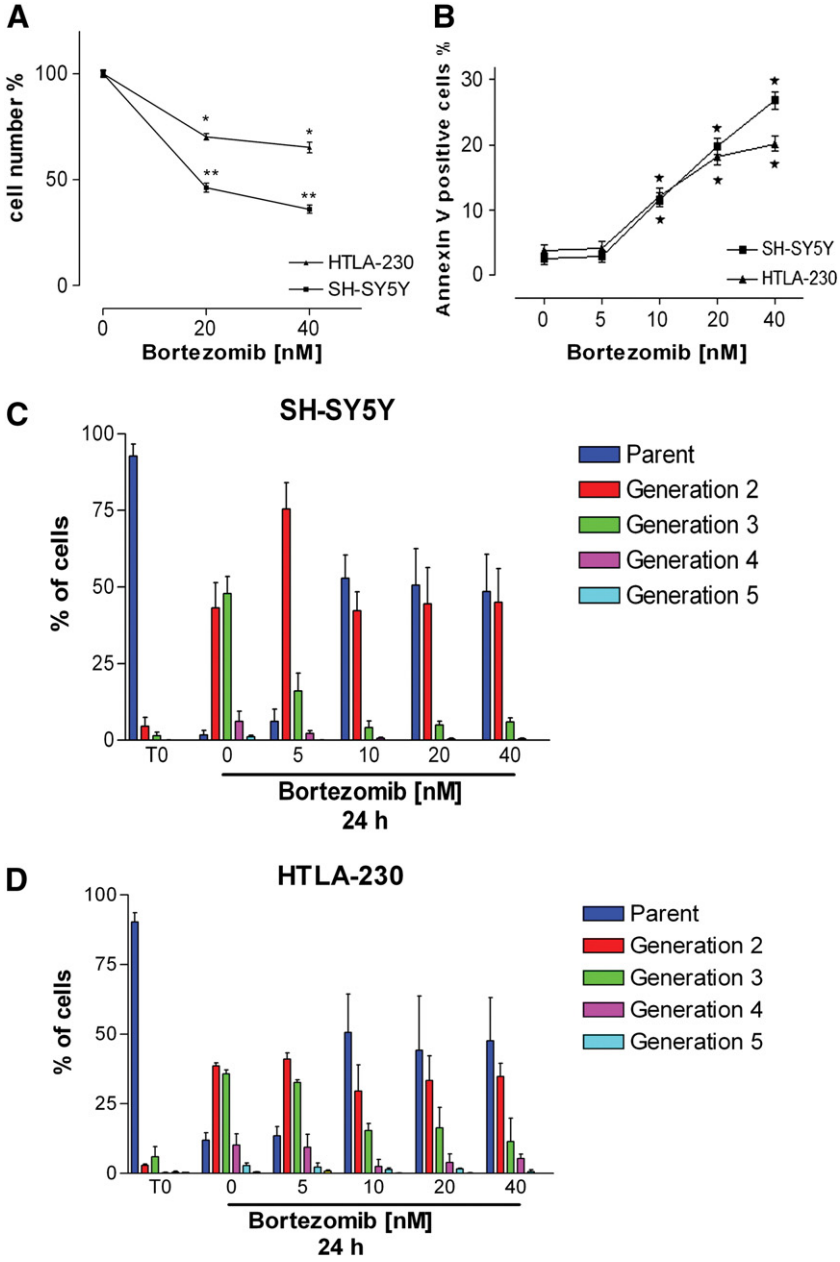

Fig. 1. Bortezomib treatment decreases cell viability and slows down proliferation rate. (A) Cells were treated with 20 and 40 nM BTZ for 24 h and viability was analyzed by MTT assay. The graph shows the mean values of three independent experiments (means ± SE); *$p < 0.001$ and **$p < 0.0001$ vs respective untreated cells. (B) Cells were treated with increasing concentrations of BTZ and the apoptotic rate (% of Annexin V positive cells) was assessed by AnnexinV/PI staining followed by FACS analysis. The graph shows the mean values of three independent experiments (means ± SE); *$p < 0.01$ vs untreated cells. (C, D) Cells were stained with CFDA-SE, treated with increasing concentration of BTZ for 24 h and analyzed by FACS. The graphs show the mean values of three independent experiments (means ± SE). Bar color meanings: blue = parental generation; orange = second generation; green = third generation; magenta = fourth generation; cyan = fifth generation.

buffer B (20% Ficoll-400, 100 mM HEPES, 300 mM KCl, 10 mM DTT and 0.1% PMSF), 5 mM MgCl2 and 20.000 cpm of a 32P-labeled oligonucleotide in a final volume of 20 μl.

After 20 min at room temperature, the reaction products were separated on a 4% non-denaturing polyacrylamide gel. Radioactivity of dried gel was detected by exposure to Kodak XAR films, and the bands were analyzed by densitometry.

2.10. Statistical analysis

The data are presented as a mean ± standard error from at least three independent experiments. The statistical significance was evaluated by one-way ANOVA followed by Dunnet post-test, or by *t*-test to compare two groups, using GraphPad Prism software (San Diego, CA, USA).

3. Results

3.1. Analysis of cell viability and proliferation after exposure to BTZ

As shown in Fig. 1A, SH-SY5Y cell viability decreased by about 55% and 65% after 24 h of 20 and 40 nM BTZ treatments respectively, in comparison to the vehicle control as revealed by MTT assay. However, HTLA-230 cells treated with the same BTZ concentrations for the same experimental time showed a decrease in viability of about 30% in comparison to the vehicle controls.

Cytofluorimetric analysis showed that 24 h treatment with 10, 20 and 40 nM BTZ induced a dose-dependent increase in Annexin V-positive SH-SY5Y cells of about 12%, 19% and 27% respectively. However, the number of Annexin V-positive HTLA-230 cells increased by 18% at 20nM BTZ treatment with no further significant increase at 40 nM (Fig. 1B).

The analysis of the proliferation rate showed that both cell lines, when untreated, proliferated strongly and after 24 h were mainly in second and third generation (as illustrated by the red and green bars respectively in Fig. 1C and D). However, the treatment with 5 nM BTZ increased the number of SH-SY5Y cells in the second generation while the same dose had no effects on HTLA-230, showing that SH-SY5Y were more sensitive to the cytostatic effect of BTZ than the HTLA-230 cells. Furthermore, WB analysis showed a dose-dependent increase of protein ubiquitination pattern in both cell lines treated with BTZ, confirming the efficacy of proteasome inhibition (data not shown).

3.2. Analysis of Nrf2-dependent genes in BTZ-treated neuroblastoma cells

In order to evaluate the antioxidant and/or detoxifying cell response, we analyzed the Nrf2 target genes. As shown in Fig. 2, in neither cell

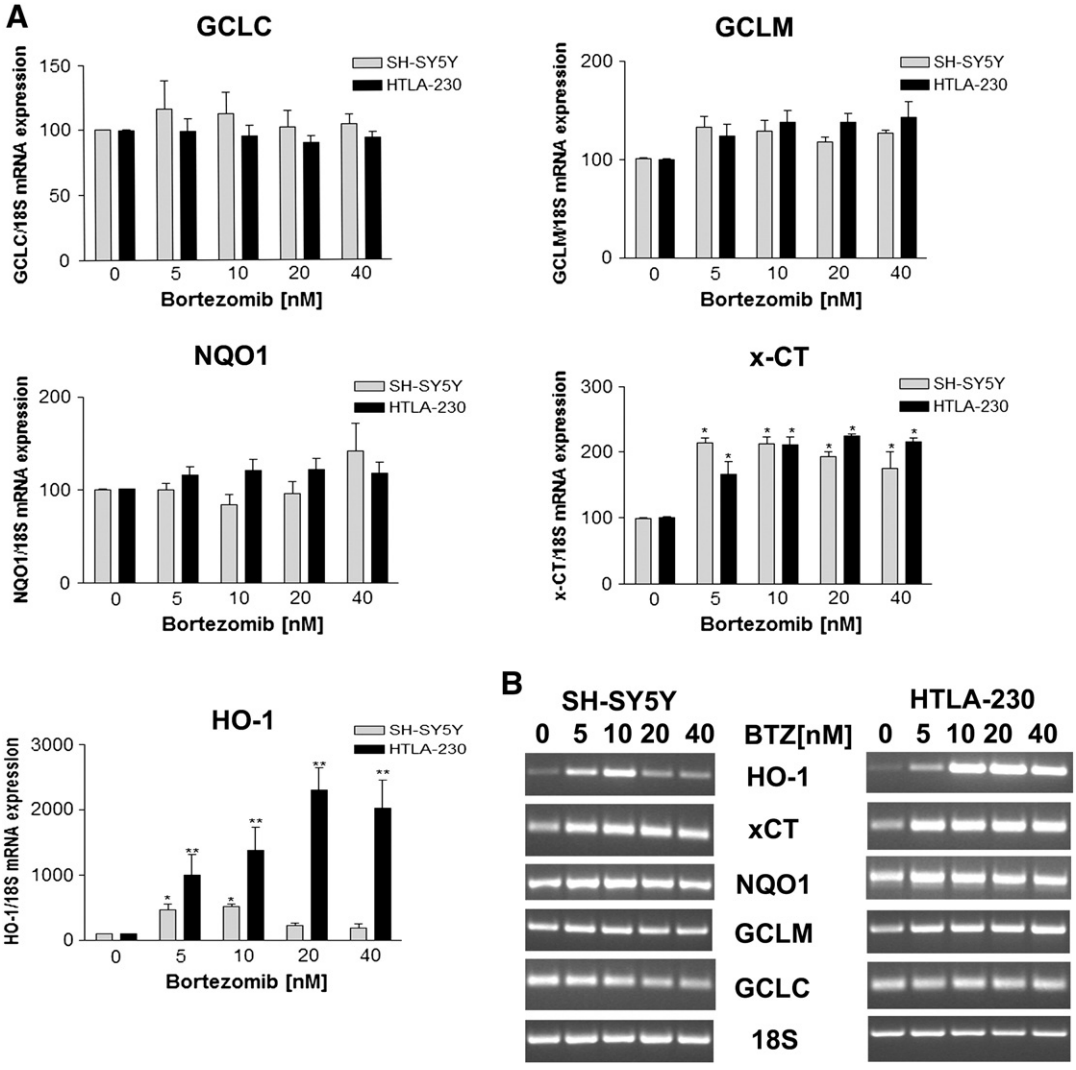

Fig. 2. Bortezomib treatment mainly increases HO-1 among the Nrf2-dependent genes. (A) RT-PCR analysis of Nrf2-dependent genes (GCLC, GCLM, NQO1, x-CT, HO-1) was performed on total RNA extracted from SH-SY5Y and HTLA-230 cell lines treated with to 5–40 nM BTZ for 24 h. PCR products were separated by electrophoresis and the relative intensities of the bands were normalized to 18S expression. The bar graphs show the mean values of three independent experiments (means ± SE); * $p < 0.05$ and ** $p < 0.01$ vs untreated cells. (B) The bands are representative of three independent experiments.

lines, after 24 h BTZ treatment (5–40 nM), were changes observed, either in the mRNA expression of heavy and light subunits of glutamyl cysteine ligase (GCLC, GCLM) or in the NQO1 expression. The transporter of cysteine, x-CT, was up-regulated in both cell lines, regardless of the BTZ concentration used (Fig. 2). However, BTZ treatment in SH-SY5Y induced HO-1 at 5 and 10 nM, by about 4-fold in comparison

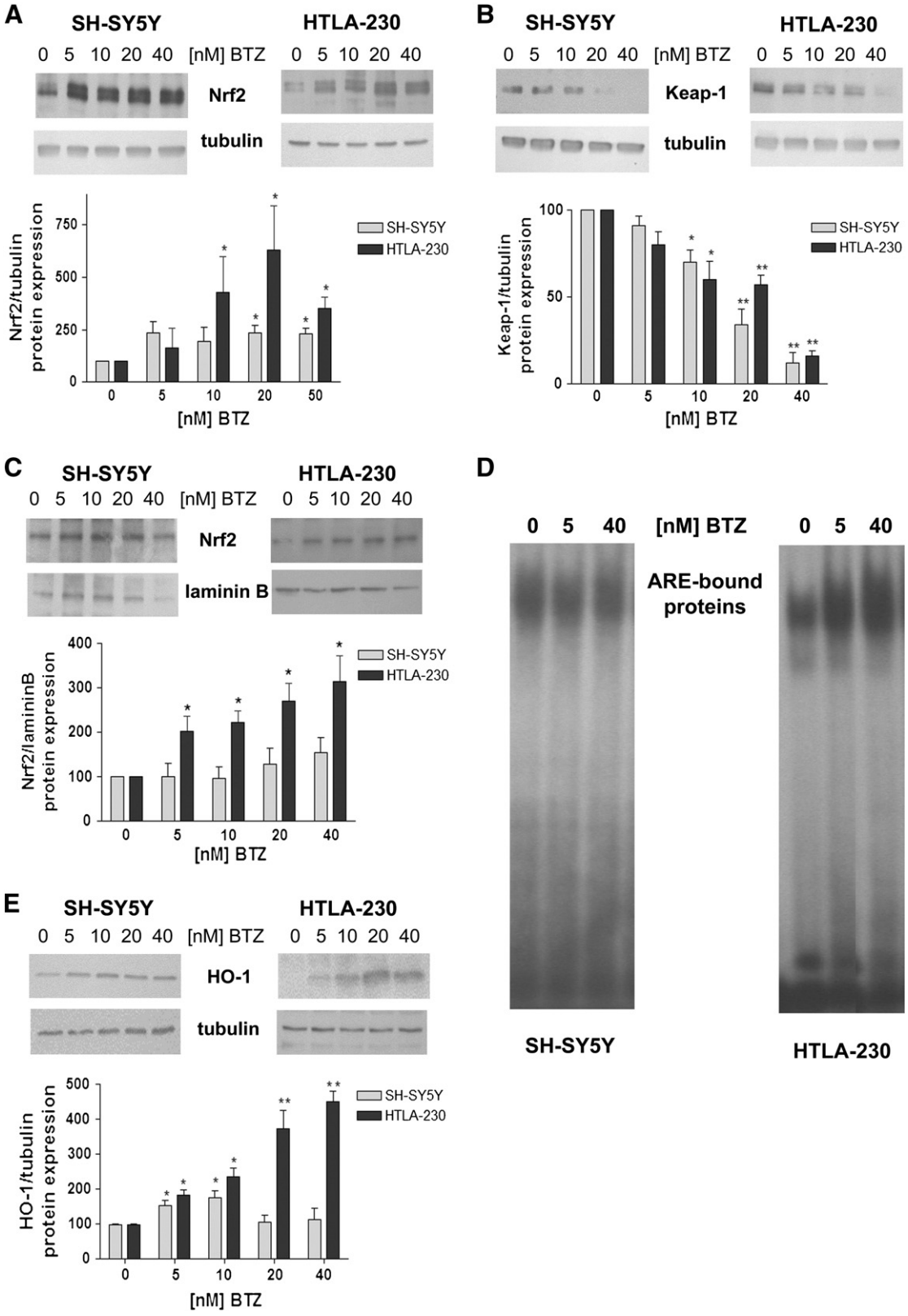

Fig. 3. Nrf2 protein level is increased in both cell lines treated with bortezomib but its ability to bind to DNA is different. Nrf2 (A), Keap-1 (B) and HO-1 (E) protein levels were evaluated in total cell lysates using a standard WB technique, checking tubulin expression as loading control. (C) Nrf2 levels of nuclear fractions have been analyzed by WB using laminin B1 as loading control; (D) nuclear protein ability to bind the DNA ARE consensus sequence was evaluated using EMSA assay. All the blots reported are from one representative experiment of three. The graphs show the mean values of three independent experiments. *$p < 0.01$ and **$p < 0.001$ vs respective untreated samples.

to untreated cells, whereas, in HTLA-230 cells, HO-1 was strongly up-regulated up to 20 fold at the highest doses of BTZ (20 and 40 nM) in comparison to the control samples (Fig. 2).

3.3. Analysis of Nrf2 and HO-1 protein level in neuroblastoma cells exposed to BTZ

Nrf2 total protein expression progressively increased in HTLA-230 cells exposed to increasing concentrations of BTZ (up to 6 fold at 20 nM BTZ) while SH-SY5Y cells showed a dose-independent increase of about 2.5 fold already at the lowest doses used (5 nM, Fig. 3A). In addition, a progressive decrease of Keap-1 protein level in both cell lines was observed (Fig. 3B). However, the analysis of nuclear fractions showed a marked dose-dependent increase of Nrf2 protein in HTLA-230 cells treated with BTZ while no significant enhancement of Nrf2 levels in the nucleus was observed in SH-SY5Y cells exposed to the same treatment (Fig. 3C). Furthermore, electrophoretic mobility shift assay (EMSA) showed that the binding of nuclear proteins to the antioxidant responsive element (ARE) consensus sequence was increased in HTLA-230 cells exposed both to the lowest and the highest doses of BTZ while the same treatments were not able to modify the ability of SH-SY5Y-derived nuclear proteins to bind to the DNA ARE sequence (Fig. 3D). Finally, HO-1 protein level was markedly increased by BTZ in a dose-dependent way in HTLA-230 (up to +350% vs untreated cells at 40 nM) while a significant up-regulation (+70% vs untreated cells) was observed only at the lowest doses used in SH-SY5Y (Fig. 3E). This was in agreement with the modulation of mRNA expression shown in Fig. 2.

3.4. Effect of HO-1 inhibition on BTZ-treated cell viability and proliferation

In order to check if HO-1 inhibition could increase cytostatic and/or cytotoxic effect of BTZ, both cell lines were treated with 2.5 μM ZnPPIX, either alone or in combination with 10 nM BTZ and the apoptotic rate was evaluated. As shown in Fig. 4, the inhibition of HO-1 activity increased the number of apoptotic HTLA-230 cells by 26% in comparison to untreated cells and by 18% in comparison to cells treated with BTZ alone. However, in SH-SY5Y cells, HO-1 activity inhibition did not influence the apoptotic effect of BTZ.

However, ZnPPIX did not change the proliferation slowdown induced by BTZ in either cell lines (data not shown).

3.5. Effect of HO-1 inhibition on p53 levels in neuroblastoma cells exposed to BTZ

WB analysis of p53 expression level revealed a dose-dependent decrease from a 50% to a70% reduction vs control in HTLA-230 cells exposed to 10–40 nM BTZ while the same BTZ treatment gradually increased the p53 expression level in SH-SY5Y cells (Fig. 5A). However, HO-1 inhibition induced by 2.5 μM ZnPPIX did not affect BTZ-dependent p53 down-regulation in HTLA-230 cells, and it had no effect on p53 over-expression induced by 10 nM BTZ in SH-SY5Y cells (Fig. 5B).

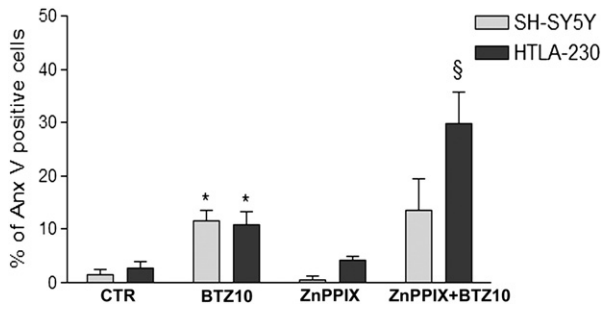

Fig. 4. Pro-apoptotic effect of BTZ is increased by treatment with HO-1 inhibitor ZnPPIX only in HTLA-230 cells. HTLA-230 and SH-SY5Y cells were co-treated with 2.5 μM ZnPPIX and 10 nM BTZ for 24 h and the apoptotic rate was assessed by AnnexinV/PI staining followed by FACS analysis. The graphs show the mean values of three independent experiments (means ± SE). *$p < 0.05$ vs respective untreated cells; § $p < 0.05$ vs BTZ-treated cells.

3.6. Effect of HO-1 inhibition on p21 expression in BTZ-treated cells

RT-PCR analysis of p21 mRNA expression revealed a marked increase (+120% vs control) in SH-SY5Y, already at the minimum dose used, without further increase at the higher doses. Moreover, HTLA-230 cells showed an increase of p21 mRNA of about 100% at 10 nM and up to 120% at 40 nM BTZ (Fig. 6A). The analysis of p21 protein level by WB showed a similar trend in both cell lines treated with BTZ (+70% vs control, already at 5 nM BTZ, with no further increases in SH-SY5Y cells and +50% vs control at 10–20–40 nM BTZ in HTLA-230 cells) (Fig. 6B).

However, in neither HTLA-230 nor SH-SY5Y cells, the co-treatment with HO-1 inhibitor 2.5 μM ZnPPIX was able to significantly affect p21 mRNA or protein over-expression induced by 10 nM BTZ (Fig. 6C and D).

3.7. Effect of HO-1 inhibition on MYCN expression in BTZ-treated HTLA-230 cells

Since MYCN amplification is one of the most important factors related to neuroblastoma aggressiveness and resistance to therapy, then we verified if BTZ treatment and HO-1 inhibition were able to influence MYCN expression. However, the expression of MYCN in SH-SY5Y cells was below the detection limits with our experimental approach and we only considered the analysis of HTLA-230 cells. Our results showed that BTZ treatment was able to reduce, in a dose-dependent way, the level of MYCN mRNA up to 35% at 40 nM BTZ in comparison to untreated cells (Fig. 7A). Moreover, the WB analysis showed that MYCN protein level decreased by 25% and 30% only at the highest BTZ doses used (20 and 40 nM respectively, Fig. 7B). However, HO-1 inhibition induced by 2.5 μM ZnPPIX had no effect on preventing the decrease of MYCN mRNA induced by BTZ (Fig. 7C). No significative changes of MYCN protein level were observed in cells treated with 10 nM BTZ or co-treated with 2.5 μM ZnPPIX (Fig. 7D).

4. Discussion

Our study identifies a crucial role of HO-1 up-regulation in high-risk neuroblastoma resistance to proteasome inhibitor-based therapy. We show that both HTLA-230 (MYCN amplified) and SH-SY5Y (MYCN non-amplified) cell lines are sensitive to the cytostatic effect of bortezomib, in line with the well-known ability of proteasome inhibition to reduce cell proliferation [25,26]. However, on the basis of the results obtained by MTT assay (cell number) and by the cytofluorimetric detection of apoptotic cells, we demonstrate that HTLA-230 are less sensitive to BTZ treatment than SH-SY5Y cells.

BTZ has already been proposed as a useful therapeutic approach to overcome chemoresistance and it has been approved as an anticancer drug both alone, for the treatment of multiple myeloma [27,28], and in combination with conventional therapies, as a chemosensitizer [29–31]. Furthermore, the efficacy of bortezomib treatment on neuroblastoma has already been proposed [32,33] but the molecular mechanism of BTZ action is not yet fully understood. In addition, more recently it has been pointed out that the role of BTZ as a general chemo-sensitizer needs to be reconsidered since its efficacy in a combined therapy is dependent on cell type and drug used. Indeed, it has been observed both a sensitizing effect of BTZ in combination with radio-therapy [34] or doxorubicin [35] and an antagonistic effect in combination with microtubule interfering-drugs [36].

In this context, we hypothesize that the efficacy of BTZ could be limited by the induction of the antioxidant Nrf2-dependent cell response, frequently activated in tumor cells after chemotherapy [37–39]. In fact, BTZ treatment is able to decrease the expression level of Keap-1, the cytosolic

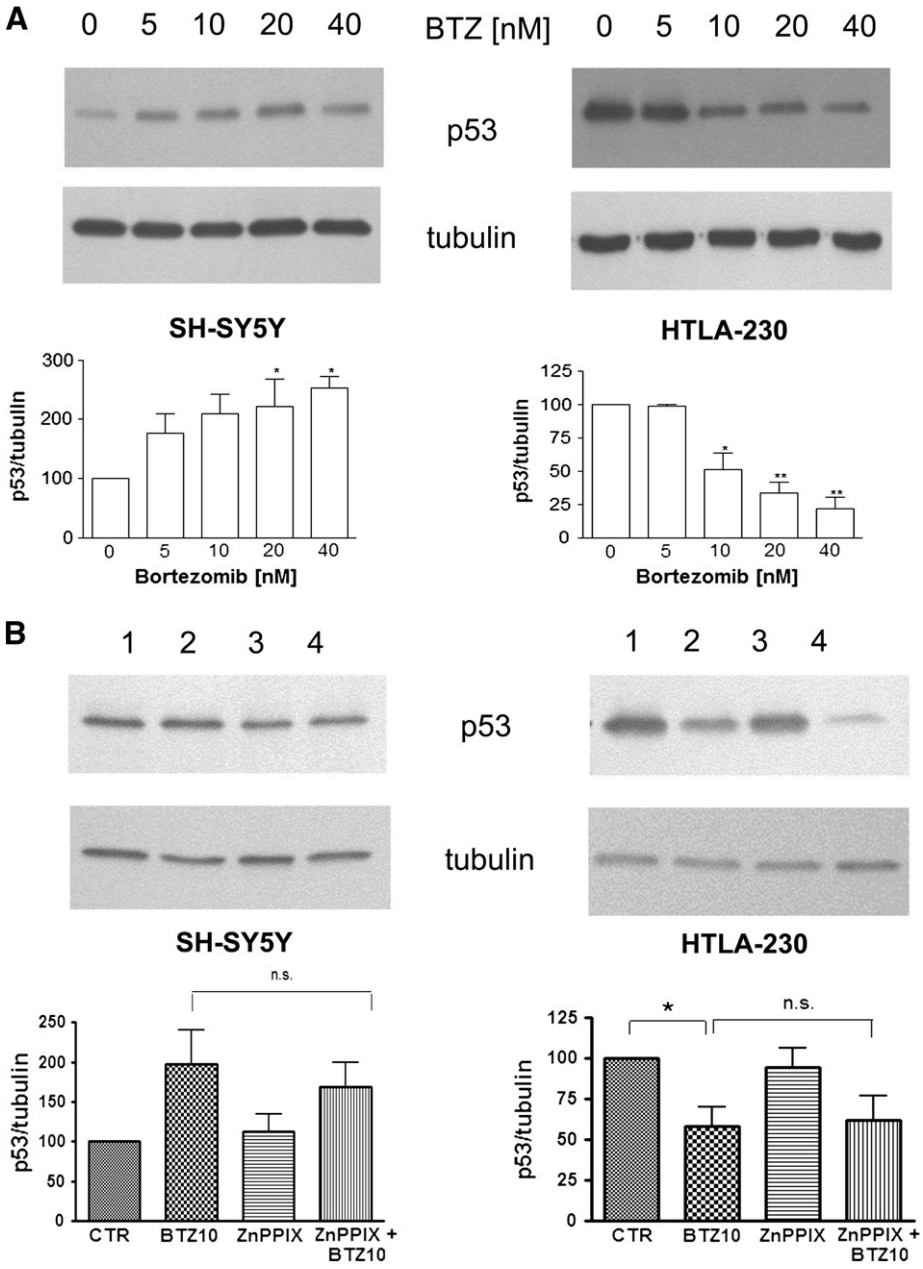

Fig. 5. p53 expression level is differently modulated in SH-SY5Y and HTLA-230 cells treated with BTZ and HO-1 inhibition does not interfere. (A) Western blot was performed on total protein extract after 24 h cell exposure to increasing concentrations of BTZ (5–40 nM), checking tubulin expression as loading control. The bar graphs show the mean values of three independent experiments (means ± SE); * $p < 0.05$ and ** $p < 0.01$ vs untreated cells. (B) p53 level was analyzed by WB on protein lysates from cells co-treated with 2.5 μM ZnPPIX and 10 nM BTZ. Lanes: 1 = control; 2 = 10 nM BTZ; 3 = 2.5 μM ZnPPIX; 4 = 2.5 μM ZnPPIX + 10 nM BTZ. All the blots reported are from one representative experiment of three. * $p < 0.05$ vs control.

inhibitor of Nrf2, thus increasing the total amount of Nrf2 in both cell lines. This is due to the particular regulation of Nrf2 by proteasome. It has been shown in other papers [40,41], indeed, that the inhibition of 26S proteasome induces a quick oxidation of Keap-1 and results in its degradation by 20S proteasome, allowing the Nrf2 translocation into the nucleus. However, in HTLA-230 cells, treated with BTZ, the nuclear Nrf2 level is increased, as is the ability of the nuclear proteins to bind the DNA ARE sequence. On the contrary, in BTZ-treated SH-SY5Y cells, the slight increase in the total Nrf2 level is not accompanied by its nuclear translocation or by the enhancement of the DNA binding activity. Nrf2 translocation to the nucleus is a complex event and is regulated by different post-transcriptional modifications that have been demonstrated to be crucial in Nrf2 nuclear shuttling failure [42,43].

Moreover, analyzing the most important Nrf2-dependent genes, we show the induction of only two target genes, x-CT and HO-1. In particular, we focus on HO-1 which results up-regulated by about 2.5 fold at the lowest doses of BTZ in SH-SY5Y and it is strongly induced up to 20 fold at 20 nM BTZ in HTLA-230 cells. Since HO-1 transcription is regulated not only by Nrf2 but also by AP-1 and NF-κB [44], we cannot exclude that in our cell model, especially as far as SH-SY5Y is concerned, the up-regulation of HO-1 observed at 5–10 nM BTZ could be due to the activation of Nrf2-independent pathways.

It is known that the induction of HO-1 exerts a strong antioxidant and antiapoptotic effect as shown in acute myeloid leukemia resistance to TNFα [45] and in the resistance of pancreatic tumors to gemcitabine [17]. In order to demonstrate the implications of HO-1 in cell resistance to BTZ cytotoxic effect, we co-treated both cell lines with 2.5 μM ZnPPIX, an inhibitor of HO-1 activity, and 10 nM BTZ, the lowest dose able to affect both cell viability and proliferation rate. The co-treatment is able to strongly increase the apoptotic rate of HTLA-230 cells, confirming

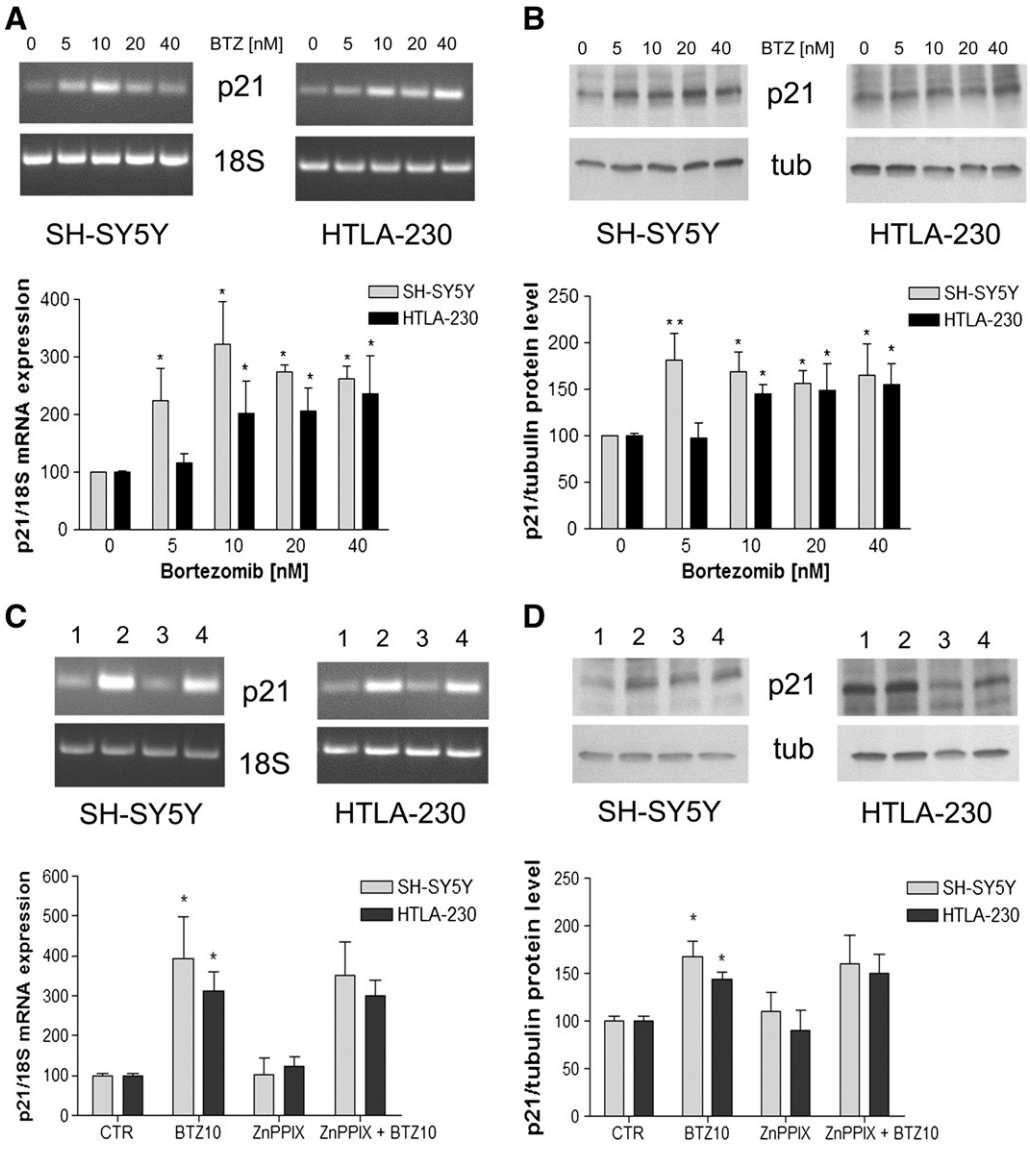

Fig. 6. p21 expression is induced by BTZ treatment in both cell lines and it is not prevented by HO-1 inhibition. (A) RT-PCR analysis of p21 was performed on total RNA extract from cells after 24 h exposure to increasing concentrations of BTZ (5–40 nM). (B) Western blot was performed on total protein extract after 24 h cell exposure to increasing concentrations of BTZ (5–40 nM), checking tubulin expression as loading control. p21mRNA expression (C) and protein level (D) was checked on cells co-treated with 2.5 μM ZnPPIX and 10 nM BTZ for 24 h. Lanes: 1 = control; 2 = 10 nM BTZ; 3 = 2.5 μM ZnPPIX; 4 = 2.5 μM ZnPPIX + 10 nM BTZ. All bands shown are representative of three independent experiments. The bar graphs show the mean values of three independent experiments (means ± SE); * $p < 0.05$ vs untreated cells; ** $p < 0.01$ vs untreated.

the role of HO-1 induction in preventing cell death. Moreover, the same co-treatment is not able to increase the apoptotic rate of SH-SY5Y cells, according to the slight increase of HO-1 expression induced by BTZ.

In order to investigate the molecular pathways that could be modulated by HO-1 and involved in the resistance to bortezomib, we studied the expression of p21, p53 and MYCN.

Here, we show that BTZ is able to induce p21 in both cell lines, to up-regulate p53 in SH-SY5Y and down-regulate it in HTLA-230 cells, and to decrease MYCN expression in HTLA-230 cells.

The proteasome-dependent regulation of p21 is well known [46] and its induction correlates with cell cycle slowdown observed in BTZ-treated cells. Although the involvement of HO-1-derived carbon monoxide in p21 up-regulation has already been confirmed [47], in our study we failed to demonstrate HO-1's involvement in BTZ-induced p21 up-regulation in both cell lines, underlining the direct involvement of 26S proteasome activity in p21 expression.

Conversely, it should be kept in mind that p53 can be degraded, not only by 26S proteasome [48], but also by 20S proteasome [49] and by a calpain-dependent cytosolic pathway [50]. In fact, we cannot exclude that the treatment of HTLA-230 with bortezomib can up-regulate other protein-degrading systems [51] in order to maintain low levels of p53 [49]. On the other hand, we demonstrate that SH-SY5Y cells, a less aggressive neuroblastoma type, react to proteasome inhibition with an expected p53 increase [48]. Interestingly, since it has been suggested that HO-1-derived carbon monoxide is able to reduce p53 expression inhibiting apoptosis in vascular smooth muscle cells [52], the high up-regulation of HO-1, induced by bortezomib in HTLA-230 cells, could contribute to the decreasing of p53 levels with the same mechanism. However, the inhibition of HO-1 activity by ZnPPIX is not able to modulate p53 levels, showing that other mechanisms must be responsible for regulating the bortezomib-induced p53 down-regulation in high-risk neuroblastoma. Moreover, cell death induced by the co-treatment is p53- and p21-independent which is in agreement with a previous study that shows bortezomib plus fenretinide induces endoplasmic reticulum stress-related apoptosis [33].

Furthermore, it has been demonstrated in literature that p53 plays a role as a negative regulator of Nrf2 [53] in that it is able to interfere with

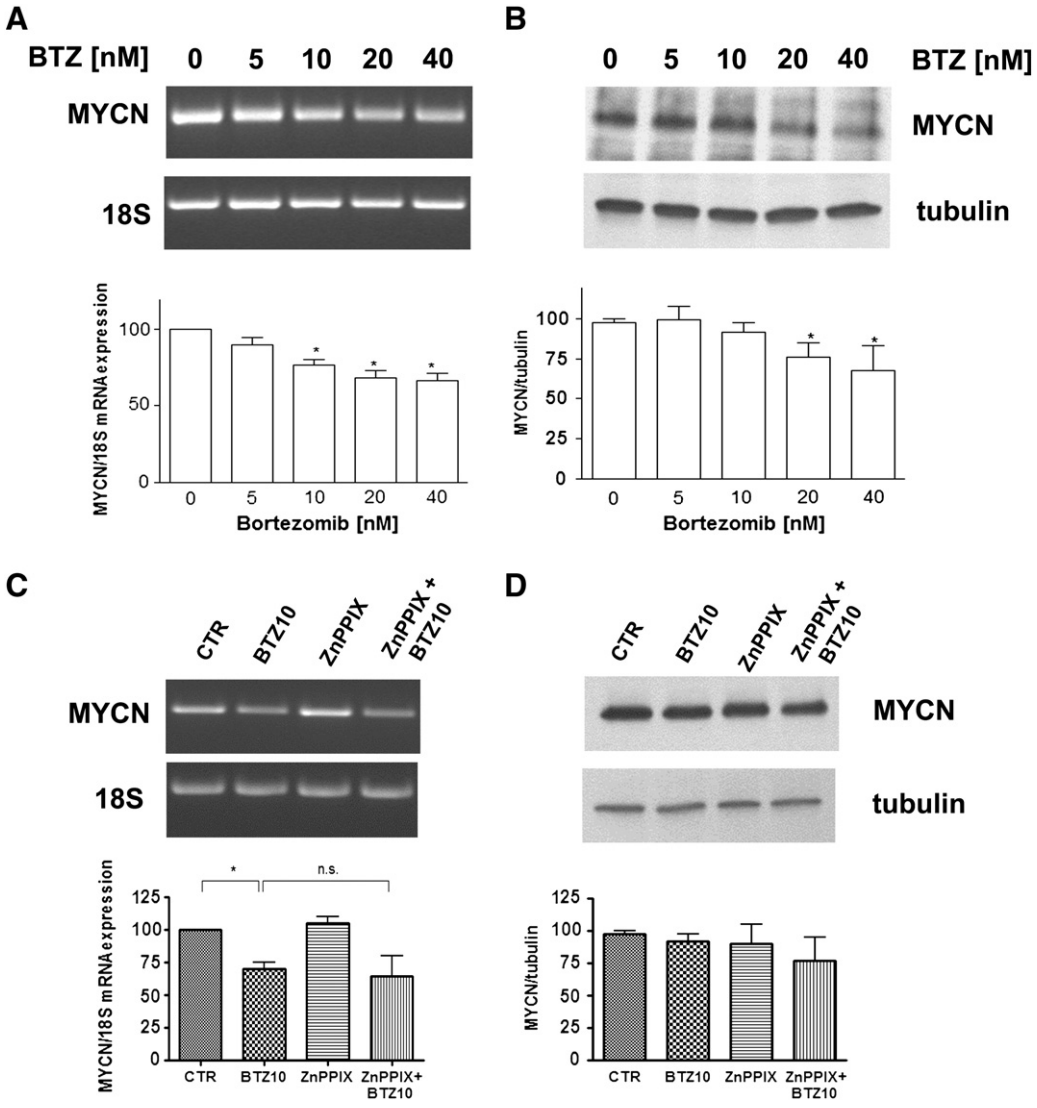

Fig. 7. Bortezomib treatment decreases MYCN expression in HTLA-230 cells, in a HO-1 independent way. RT-PCR analysis (A) and WB analysis (B) of MYCN were performed on HTLA-230 cell exposed to 5–40 nM BTZ for 24 h and after co-treatment with 2.5 μM ZnPPIX and 10 nM BTZ (C and D). The bands are representative of three independent experiments. All the bar graphs show the mean values of three independent experiments (means ± SE); * $p < 0.05$ vs untreated cells.

the ability of Nrf2 to bind to the DNA ARE sequence. Therefore, we can speculate that in HTLA-230 cells the p53 decrease might favor Nrf2 binding to the DNA and HO-1 transcription. On the contrary, the loss of the ability of Nrf2 to bind to the DNA, observed in SH-SY5Y cells, could be related to the p53 increase induced by bortezomib.

Finally, since the up-regulation of proto-oncogene MYCN in NB cells treated with proteasome inhibitors has been shown [54], we have investigated MYCN expression in HTLA-230, a prototype of MYCN amplified NB cells. In our model, BTZ treatment induces MYCN down-regulation that could contribute to the reduction of p53 expression, leading to a major cell survival. In fact, it has been shown that in SHEP Tet21N cells, in which MYCN expression can be switched on and off, MYCN expression correlates with p53 expression and, when up-regulated, leads to apoptosis [55]. Moreover, MYCN down-regulation induced by BTZ seems to be independent from HO-1 since it is not prevented by HO-1 inhibition induced by ZnPPIX.

However, it is increasingly evident from literature that MYCN regulation is highly complex and regulates NB biology through a wide variety of direct or indirect target genes not only in MYCN amplified cells, but also in non-amplified cells that express low levels of MYCN protein [56]. Therefore, the role of MYCN in the sensitivity of neuroblastoma cells to proteasome inhibitors deserves more investigation.

5. Conclusion

We have provided evidence that HO-1 up-regulation, playing a strong anti-apoptotic and pro-surviving role, characterizes the increase of resistance to proteasome-inhibition based therapy in high-risk MYCN-amplified neuroblastoma. Indeed, HO-1 inhibition, achieved using ZnPPIX, significantly improves the pro-apoptotic effect of the proteasome inhibitor and this combined therapy allows the reduction in the doses of BTZ used. Thus, we propose HO-1 as a marker of chemoresistance. The detection of its over-expression could direct the therapy towards the use of HO-1 inhibitors in order to improve the efficacy of chemotherapy.

Acknowledgements

Grants from MIUR-PRIN 2009M8FKBB_002, Fondazione CARIGE and Genoa University.

References

[1] J.R. Park, A. Eggert, H. Caron, Neuroblastoma: biology, prognosis, and treatment, Hematol. Oncol. Clin. North Am. 24 (2010) 65–86.
[2] M. Ohira, A. Nakagawara, Global genomic and RNA profiles for novel risk stratification of neuroblastoma, Cancer Sci. 101 (2010) 2295–2301.

[3] X.X. Tang, M.E. Robinson, J.S. Riceberg, D.Y. Kim, B. Kung, T.B. Titus, S. Hayashi, A.W. Flake, D. Carpentieri, N. Ikegaki, Favorable neuroblastoma genes and molecular therapeutics of neuroblastoma, Clin. Cancer Res. 10 (2004) 5837–5844.
[4] G.K. Balendiran, R. Dabur, D. Fraser, The role of glutathione in cancer, Cell Biochem. Funct. 22 (2004) 343–352.
[5] X.J. Wang, Z. Sun, N.F. Villeneuve, S. Zhang, F. Zhao, Y. Li, W. Chen, X. Yi, W. Zheng, G.T. Wondrak, P.K. Wong, D.D. Zhang, Nrf2 enhances resistance of cancer cells to chemotherapeutic drugs, the dark side of Nrf2, Carcinogenesis 29 (2008) 1235–1243.
[6] A. Lau, N.F. Villeneuve, Z. Sun, P.K. Wong, D.D. Zhang, Dual roles of Nrf2 in cancer, Pharmacol. Res. 58 (2008) 262–270.
[7] G.M. Trakshel, M.D. Maines, Multiplicity of heme oxygenase isozymes. HO-1 and HO-2 are different molecular species in rat and rabbit, J. Biol. Chem. 264 (1989) 1323–1328.
[8] M.D. Maines, Heme oxygenase: function, multiplicity, regulatory mechanisms, and clinical applications, FASEB J. 2 (1988) 2557–2568.
[9] S.M. Keyse, R.M. Tyrrell, Heme oxygenase is the major 32-kDa stress protein induced in human skin fibroblasts by UVA radiation, hydrogen peroxide, and sodium arsenite, Proc. Natl. Acad. Sci. U. S. A. 86 (1989) 99–103.
[10] J. Alam, S. Shibahara, A. Smith, Transcriptional activation of the heme oxygenase gene by heme and cadmium in mouse hepatoma cells, J. Biol. Chem. 264 (1989) 6371–6375.
[11] S. Patriarca, A.L. Furfaro, L. Cosso, E. Pesce Maineri, E. Balbis, C. Domenicotti, M. Nitti, D. Cottalasso, U.M. Marinari, M.A. Pronzato, N. Traverso, Heme oxygenase 1 expression in rat liver during ageing and ethanol intoxication, Biogerontology 8 (2007) 365–372.
[12] R. Stocker, Y. Yamamoto, A.F. McDonagh, A.N. Glazer, B.N. Ames, Bilirubin is an antioxidant of possible physiological importance, Science 235 (1987) 1043–1046.
[13] A. Jozkowicz, H. Was, J. Dulak, Heme oxygenase-1 in tumors: is it a false friend? Antioxid. Redox Signal. 9 (2007) 2099–2117.
[14] A.I. Goodman, M. Choudhury, J.L. da Silva, M.L. Schwartzman, N.G. Abraham, Overexpression of the heme oxygenase gene in renal cell carcinoma, Proc. Soc. Exp. Biol. Med. 214 (1997) 54–61.
[15] M.D. Maines, P.A. Abrahamsson, Expression of heme oxygenase-1 (HSP32) in human prostate: normal, hyperplastic, and tumor tissue distribution, Urology 47 (1996) 727–733.
[16] P.O. Berberat, Z. Dambrauskas, A. Gulbinas, T. Giese, N. Giese, B. Kunzli, F. Autschbach, S. Meuer, M.W. Buchler, H. Friess, Inhibition of heme oxygenase-1 increases responsiveness of pancreatic cancer cells to anticancer treatment, Clin. Cancer Res. 11 (2005) 3790–3798.
[17] P. Nuhn, B.M. Kunzli, R. Hennig, T. Mitkus, T. Ramanauskas, R. Nobiling, S.C. Meuer, H. Friess, P.O. Berberat, Heme oxygenase-1 and its metabolites affect pancreatic tumor growth in vivo, Mol. Cancer 8 (2009) 37.
[18] A.L. Furfaro, J.R. Macay, B. Marengo, M. Nitti, A. Parodi, D. Fenoglio, U.M. Marinari, M.A. Pronzato, C. Domenicotti, N. Traverso, Resistance of neuroblastoma GI-ME-N cell line to glutathione depletion involves Nrf2 and heme oxygenase-1, Free Radic. Biol. Med. 52 (2012) 488–496.
[19] S.A. Rushworth, K.M. Bowles, D.J. MacEwan, High basal nuclear levels of Nrf2 in acute myeloid leukemia reduces sensitivity to proteasome inhibitors, Cancer Res. 71 (2011) 1999–2009.
[20] S.T. Pellom Jr., A. Shanker, Development of proteasome inhibitors as therapeutic drugs, J. Clin. Cell. Immunol. S5 (2012) 5.
[21] M.A. Weniger, E.G. Rizzatti, P. Perez-Galan, D. Liu, Q. Wang, P.J. Munson, N. Raghavachari, T. White, M.M. Tweito, K. Dunleavy, Y. Ye, W.H. Wilson, A. Wiestner, Treatment-induced oxidative stress and cellular antioxidant capacity determine response to bortezomib in mantle cell lymphoma, Clin. Cancer Res. 17 (2011) 5101–5112.
[22] T. Mujtaba, Q.P. Dou, Advances in the understanding of mechanisms and therapeutic use of bortezomib, Discov. Med. 12 (2011) 471–480.
[23] S. Urbani, R. Caporale, L. Lombardini, A. Bosi, R. Saccardi, Use of CFDA-SE for evaluating the in vitro proliferation pattern of human mesenchymal stem cells, Cytotherapy 8 (2006) 243–253.
[24] M.K. Kwak, K. Itoh, M. Yamamoto, T.W. Kensler, Enhanced expression of the transcription factor Nrf2 by cancer chemopreventive agents: role of antioxidant response element-like sequences in the nrf2 promoter, Mol. Cell. Biol. 22 (2002) 2883–2892.
[25] S. Frankland-Searby, S.R. Bhaumik, The 26S proteasome complex: an attractive target for cancer therapy, Biochim. Biophys. Acta 1825 (2012) 64–76.
[26] W.K. Wu, C.H. Cho, C.W. Lee, K. Wu, D. Fan, J. Yu, J.J. Sung, Proteasome inhibition: a new therapeutic strategy to cancer treatment, Cancer Lett. 293 (2010) 15–22.
[27] T. Hideshima, K.C. Anderson, Biologic impact of proteasome inhibition in multiple myeloma cells—from the aspects of preclinical studies, Semin. Hematol. 49 (2012) 223–227.
[28] P. Moreau, P.G. Richardson, M. Cavo, R.Z. Orlowski, J.F. San Miguel, A. Palumbo, J.L. Harousseau, Proteasome inhibitors in multiple myeloma: 10 years later, Blood 120 (2012) 947–959.
[29] J.A. Muscal, P.A. Thompson, T.M. Horton, A.M. Ingle, C.H. Ahern, R.M. McGovern, J.M. Reid, M.M. Ames, I. Espinoza-Delgado, B.J. Weigel, S.M. Blaney, A phase I trial of vorinostat and bortezomib in children with refractory or recurrent solid tumors: a Children's Oncology Group phase I consortium study (ADVL0916), Pediatr. Blood Cancer 60 (2013) 390–395.
[30] W. Blum, S. Schwind, S.S. Tarighat, S. Geyer, A.K. Eisfeld, S. Whitman, A. Walker, R. Klisovic, J.C. Byrd, R. Santhanam, H. Wang, J.P. Curfman, S.M. Devine, S. Jacob, C. Garr, C. Kefauver, D. Perrotti, K.K. Chan, C.D. Bloomfield, M.A. Caligiuri, M.R. Grever, R. Garzon, G. Marcucci, Clinical and pharmacodynamic activity of bortezomib and decitabine in acute myeloid leukemia, Blood 119 (2012) 6025–6031.
[31] A.R. Mato, T. Feldman, A. Goy, Proteasome inhibition and combination therapy for non-Hodgkin's lymphoma: from bench to bedside, Oncologist 17 (2012) 694–707.
[32] C. Brignole, D. Marimpietri, F. Pastorino, B. Nico, D. Di Paolo, M. Cioni, F. Piccardi, M. Cilli, A. Pezzolo, M.V. Corrias, V. Pistoia, D. Ribatti, G. Pagnan, M. Ponzoni, Effect of bortezomib on human neuroblastoma cell growth, apoptosis, and angiogenesis, J. Natl. Cancer Inst. 98 (2006) 1142–1157.
[33] G. Pagnan, D. Di Paolo, R. Carosio, F. Pastorino, D. Marimpietri, C. Brignole, A. Pezzolo, M. Loi, L.J. Galietta, F. Piccardi, M. Cilli, B. Nico, D. Ribatti, V. Pistoia, M. Ponzoni, The combined therapeutic effects of bortezomib and fenretinide on neuroblastoma cells involve endoplasmic reticulum stress response, Clin. Cancer Res. 15 (2009) 1199–1209.
[34] C. Rae, M. Tesson, J.W. Babich, M. Boyd, R.J. Mairs, Radiosensitization of noradrenaline transporter-expressing tumour cells by proteasome inhibitors and the role of reactive oxygen species, EJNMMI Res. 3 (2013) 73.
[35] B.Y. Du, W. Song, L. Bai, Y. Shen, S.Y. Miao, L.F. Wang, Synergistic effects of combination treatment with bortezomib and doxorubicin in human neuroblastoma cell lines, Chemotherapy 58 (2012) 44–51.
[36] F. Rapino, I. Naumann, S. Fulda, Bortezomib antagonizes microtubule-interfering drug-induced apoptosis by inhibiting G2/M transition and MCL-1 degradation, Cell Death Dis. 4 (2013) e925.
[37] T. Ohta, K. Iijima, M. Miyamoto, I. Nakahara, H. Tanaka, M. Ohtsuji, T. Suzuki, A. Kobayashi, J. Yokota, T. Sakiyama, T. Shibata, M. Yamamoto, S. Hirohashi, Loss of Keap1 function activates Nrf2 and provides advantages for lung cancer cell growth, Cancer Res. 68 (2008) 1303–1309.
[38] T. Jiang, N. Chen, F. Zhao, X.J. Wang, B. Kong, W. Zheng, D.D. Zhang, High levels of Nrf2 determine chemoresistance in type II endometrial cancer, Cancer Res. 70 (2010) 5486–5496.
[39] T. Shibata, A. Kokubu, M. Gotoh, H. Ojima, T. Ohta, M. Yamamoto, S. Hirohashi, Genetic alteration of Keap1 confers constitutive Nrf2 activation and resistance to chemotherapy in gallbladder cancer, Gastroenterology 135 (2008) 1358–1368(1368 e1-4).
[40] S.J. Chapple, R.C. Siow, G.E. Mann, Crosstalk between Nrf2 and the proteasome: therapeutic potential of Nrf2 inducers in vascular disease and aging, Int. J. Biochem. Cell Biol. 44 (2012) 1315–1320.
[41] K. Taguchi, H. Motohashi, M. Yamamoto, Molecular mechanisms of the Keap1-Nrf2 pathway in stress response and cancer evolution, Genes Cells 16 (2011) 123–140.
[42] H.C. Huang, T. Nguyen, C.B. Pickett, Phosphorylation of Nrf2 at Ser-40 by protein kinase C regulates antioxidant response element-mediated transcription, J. Biol. Chem. 277 (2002) 42769–42774.
[43] Y. Kawai, L. Garduno, M. Theodore, J. Yang, I.J. Arinze, Acetylation–deacetylation of the transcription factor Nrf2 (nuclear factor erythroid 2-related factor 2) regulates its transcriptional activity and nucleocytoplasmic localization, J. Biol. Chem. 286 (2011) 7629–7640.
[44] E.O. Farombi, Y.J. Surh, Heme oxygenase-1 as a potential therapeutic target for hepatoprotection, J. Biochem. Mol. Biol. 39 (2006) 479–491.
[45] S.A. Rushworth, K.M. Bowles, P. Raninga, D.J. MacEwan, NF-kappaB-inhibited acute myeloid leukemia cells are rescued from apoptosis by heme oxygenase-1 induction, Cancer Res. 70 (2010) 2973–2983.
[46] S. Chen, J.L. Blank, T. Peters, X.J. Liu, D.M. Rappoli, M.D. Pickard, S. Menon, J. Yu, D.L. Driscoll, T. Lingaraj, A.L. Burkhardt, W. Chen, K. Garcia, D.S. Sappal, J. Gray, P. Hales, P.J. Leroy, J. Ringeling, C. Rabino, J.J. Spelman, J.P. Morgenstern, E.S. Lightcap, Genome-wide siRNA screen for modulators of cell death induced by proteasome inhibitor bortezomib, Cancer Res. 70 (2010) 4318–4326.
[47] C.I. Schwer, M. Mutschler, P. Stoll, U. Goebel, M. Humar, A. Hoetzel, R. Schmidt, Carbon monoxide releasing molecule-2 inhibits pancreatic stellate cell proliferation by activating p38 mitogen-activated protein kinase/heme oxygenase-1 signaling, Mol. Pharmacol. 77 (2010) 660–669.
[48] E. Tai, S. Benchimol, TRIMming p53 for ubiquitination, Proc. Natl. Acad. Sci. U. S. A. 106 (2009) 11431–11432.
[49] P. Tsvetkov, N. Reuven, Y. Shaul, Ubiquitin-independent p53 proteasomal degradation, Cell Death Differ. 17 (2010) 103–108.
[50] M. Pariat, S. Carillo, M. Molinari, C. Salvat, L. Debussche, L. Bracco, J. Milner, M. Piechaczyk, Proteolysis by calpains: a possible contribution to degradation of p53, Mol. Cell. Biol. 17 (1997) 2806–2815.
[51] J.S. Gelman, J. Sironi, I. Berezniuk, S. Dasgupta, L.M. Castro, F.C. Gozzo, E.S. Ferro, L.D. Fricker, Alterations of the intracellular peptidome in response to the proteasome inhibitor bortezomib, PLoS One 8 (2013) e53263.
[52] X.M. Liu, G.B. Chapman, K.J. Peyton, A.I. Schafer, W. Durante, Carbon monoxide inhibits apoptosis in vascular smooth muscle cells, Cardiovasc. Res. 55 (2002) 396–405.
[53] R. Faraonio, P. Vergara, D. Di Marzo, M.G. Pierantoni, M. Napolitano, T. Russo, F. Cimino, p53 suppresses the Nrf2-dependent transcription of antioxidant response genes, J. Biol. Chem. 281 (2006) 39776–39784.
[54] P. Bonvini, P. Nguyen, J. Trepel, L.M. Neckers, In vivo degradation of N-myc in neuroblastoma cells is mediated by the 26S proteasome, Oncogene 16 (1998) 1131–1139.
[55] L. Chen, N. Iraci, S. Gherardi, L.D. Gamble, K.M. Wood, G. Perini, J. Lunec, D.A. Tweddle, p53 is a direct transcriptional target of MYCN in neuroblastoma, Cancer Res. 70 (2010) 1377–1388.
[56] E. Bell, L. Chen, T. Liu, G.M. Marshall, J. Lunec, D.A. Tweddle, MYCN oncoprotein targets and their therapeutic potential, Cancer Lett. 293 (2010) 144–157.